

Biomarker Investigation using Multiple Brain Measures from Magnetic Resonance Imaging through Explainable Artificial Intelligence in Alzheimer’s Disease Classification

SUPPLEMENTARY FIGURES AND TABLES

Table S1. Full list of acronyms.

GENERAL ACRONYMS					
AAL	Automated Anatomical Labeling atlas	FSL	FMRIB Software Library	OASIS-3	Third release of the Open Access Series of Imaging Studies
AD	Alzheimer's Disease	GAP	Global Average Pooling	ReLU	Rectified Linear Unit
ADNI	Alzheimer's Disease Neuroimaging Initiative	GCN	Graph Convolutional Network	ResNet18	Residual Network with 18 layers
AI	Artificial Intelligence	GNN	Graph Neural Network	RV	Relevance Value
AUC	Area Under the Curve	GPC	Graph Path Convolution	SE	Squeeze-and-Excitation
BC-GCN-SE	Brain-Connectivity-Graph-Convolutional-Network with Squeeze-and-Excitation	Grad-CAM	Gradient-weighted Class Activation Mapping	SMOTE	Synthetic Minority Over-sampling Technique
CAM	Class Activation Mapping	GRAPPA	Generalized Autocalibrating Partially Parallel Acquisition	sMRI	structural Magnetic Resonance Imaging

CDR	Clinical Dementia Rating	HC	Healthy Controls	SPIDER-NET	Software Package Ideal for Deriving Enhanced Representations of brain NETWORKs
CNN	Convolutional Neural Network	HOA	Harvard-Oxford Atlas	TE	Echo Time
DL	Deep Learning	IQR	Interquartile Range	TI	Inversion Time
DMN	Default Mode Network	isoWU	isotropic Weighted Undersampling	TNR	True Negative Rate
dMRI	diffusion Magnetic Resonance Imaging	ML	Machine Learning	TPR	True Positive Rate
DTI	Diffusion Tensor Imaging	MPRAGE	Magnetization Prepared Rapid Acquisition Gradient Echo	TR	Repetition Time
EP	Edge Pooling	MRI	Magnetic Resonance Imaging	WM	White Matter
FC	Fully Connected	NeMo	Network Modification	XAI	Explainable Artificial Intelligence
FOV	Field of View	NP	Node Pooling		

BRAIN PARCEL ACRONYMS OF THE HARVARD-OXFORD ATLAS COMBINED WITH THE AUTOMATED ANATOMICAL LABELING ATLAS

AC	Cingulate Gyrus, anterior division	HG	Heschls Gyrus	PO	Parietal Operculum Cortex
AG	Angular Gyrus	Hip	Hippocampus	PostCG	Postcentral Gyrus
aITG	Inferior Temporal Gyrus, anterior division	IC	Insular Cortex	PP	Planum Polare
Amg	Amygdala	ICC	Intracalcarine Cortex	pPaHC	Parahippocampal Gyrus, posterior division
aMTG	Middle Temporal Gyrus, anterior division	IFG_oper	Inferior Frontal Gyrus, pars opercularis	PreCG	Precentral Gyrus

aPaHC	Parahippocampal Gyrus, anterior division	iLOC	Lateral Occipital Cortex, inferior division	PrCun	Precuneous Cortex
aSMG	Supramarginal Gyrus, anterior division	LG	Lingual Gyrus	pSMG	Supramarginal Gyrus, posterior division
aSTG	Superior Temporal Gyrus, anterior division	MedFC	Frontal Medial Cortex	pSTG	Superior Temporal Gyrus, posterior division
aTFusC	Temporal Fusiform Cortex, anterior division	MidFG	Middle Frontal Gyrus	PT	Planum Temporale
BSt	Brain-Stem	NAcc	Accumbens	Pu	Putamen
CaN	Caudate	OFusG	Occipital Fusiform Gyrus	SCC	Supracalcarine Cortex
Cereb1	Cerebelum Crus1	OP	Occipital Pole	SFG	Superior Frontal Gyrus
Cereb2	Cerebelum Crus2	PaCiG	Paracingulate Gyrus	sIFG_tri	Inferior Frontal Gyrus, pars triangularis
Cereb3	Cerebelum 3	Pal	Pallidum	sLOC	Lateral Occipital Cortex, superior division
Cereb45	Cerebelum 4 5	PC	Cingulate Gyrus, posterior division	SMA	Juxtapositional Lobule Cortex - formerly Supplementary Motor Cortex
Cereb6	Cerebelum 6	pITG	Inferior Temporal Gyrus, posterior division	SPL	Superior Parietal Lobule
Cereb7	Cerebelum 7b	pMTG	Middle Temporal Gyrus, posterior division	SubCalC	Subcallosal Cortex
Cereb8	Cerebelum 8	Tha	Thalamus	TOFusC	Temporal Occipital Fusiform Cortex
Cereb9	Cerebelum 9	toITG	Inferior Temporal Gyrus, temporooccipital part	TP	Temporal Pole
Cereb10	Cerebelum 10	toMTG	Middle Temporal Gyrus, temporooccipital part	Ver12	Vermis 1 2

CO	Central Opercular Cortex	Ver3	Vermis 3	Ver7	Vermis 7
Cuneal	Cuneal Cortex	Ver45	Vermis 4 5	Ver8	Vermis 8
FO	Frontal Operculum Cortex	Ver6	Vermis 6	Ver9	Vermis 9
FOrb	Frontal Orbital Cortex	pTFusC	Temporal Fusiform Cortex, posterior division	Ver10	Vermis 10
FP	Frontal Pole				

Table S2. Statistical analysis of differences in Grad-CAM based RV measures between the AD and HC groups for all brain parcels relative to the ResNet18 and BC-GCN-SE models.

ResNet18 (3D T1-weighted volumes)				BC-GCN-SE (Structural connectivity matrices)			
Parcel	Adjust. p	Parcel	Adjust. p	Parcel	Adjust. p	Parcel	Adjust. p
AC	<0.001 ***	AG_l	0.202	AC	1.000	AG_l	0.268
AG_r	<0.001 ***	Amg_l	<0.001 ***	AG_r	0.025 *	Amg_l	0.508
Amg_r	<0.001 ***	aPaHC_l	<0.001 ***	Amg_r	0.017 *	aPaHC_l	0.323
aPaHC_r	<0.001 ***	aSTG_l	1.000	aPaHC_r	0.268	aSTG_l	0.038 *
aSTG_r	0.464	aSMG_l	0.206	aSTG_r	0.073	aSMG_l	0.464
aSMG_r	1.000	aTFusC_l	<0.001 ***	aSMG_r	0.031 *	aTFusC_l	0.415
aTFusC_r	<0.001 ***	BSt	0.024 *	aTFusC_r	0.014 *	BSt	<0.001 ***
CaN_l	<0.001 ***	CaN_r	<0.001 ***	CaN_l	0.291	CaN_r	0.006 **
Cereb1_l	<0.001 ***	Cereb1_r	0.889	Cereb1_l	1.000	Cereb1_r	0.028 *
Cereb2_l	1.000	Cereb2_r	<0.001 ***	Cereb2_l	1.000	Cereb2_r	0.034 *
Cereb3_l	1.000	Cereb3_r	1.000	Cereb3_l	0.909	Cereb3_r	1.000
Cereb45_l	0.227	Cereb45_r	1.000	Cereb45_l	1.000	Cereb45_r	1.000
Cereb6_l	<0.001 ***	Cereb6_r	0.001 **	Cereb6_l	1.000	Cereb6_r	1.000
Cereb7_l	<0.001 ***	Cereb7_r	1.000	Cereb7_l	1.000	Cereb7_r	1.000

Cereb8_l	<0.001 ***	Cereb8_r	<0.001 ***	Cereb8_l	1.000	Cereb8_r	1.000
Cereb9_l	<0.001 ***	Cereb9_r	<0.001 ***	Cereb9_l	1.000	Cereb9_r	1.000
Cereb10_l	1.000	Cereb10_r	0.074	Cereb10_l	0.103	Cereb10_r	0.186
CO_l	1.000	CO_r	1.000	CO_l	1.000	CO_r	1.000
Cuneal_l	<0.001 ***	Cuneal_r	<0.001 ***	Cuneal_l	0.111	Cuneal_r	0.016 *
FO_l	<0.001 ***	FO_r	<0.001 ***	FO_l	0.296	FO_r	0.001 **
FOrb_l	0.756	FOrb_r	1.000	FOrb_l	0.124	FOrb_r	1.000
FP_l	<0.001 ***	FP_r	<0.001 ***	FP_l	0.908	FP_r	0.018 *
HG_l	0.540	HG_r	0.486	HG_l	0.281	HG_r	0.016 *
Hip_l	<0.001 ***	Hip_r	<0.001 ***	Hip_l	1.000	Hip_r	1.000
IC_l	0.122	IC_r	<0.001 ***	IC_l	1.000	IC_r	1.000
ICC_l	1.000	ICC_r	1.000	ICC_l	0.128	ICC_r	0.031 *
IFG_oper_l	<0.001 ***	IFG_oper_r	<0.001 ***	IFG_oper_l	0.142	IFG_oper_r	1.000
IFG_tri_l	<0.001 ***	IFG_tri_r	<0.001 ***	IFG_tri_l	0.018 *	IFG_tri_r	0.044 *
iLOC_l	1.000	iLOC_r	0.094	iLOC_l	0.129	iLOC_r	<0.001 ***
LG_l	1.000	LG_r	1.000	LG_l	1.000	LG_r	0.044 *
MedFC	<0.001 ***	MidFG_l	<0.001 ***	MedFC	0.006 **	MidFG_l	1.000
MidFG_r	<0.001 ***	NAcc_l	<0.001 ***	MidFG_r	0.118	NAcc_l	0.002 **
NAcc_r	1.000	OFusG_l	0.026 *	NAcc_r	0.015 *	OFusG_l	1.000
OFusG_r	1.000	OP_l	<0.001 ***	OFusG_r	0.018 *	OP_l	0.701
OP_r	<0.001 ***	PaCiG_l	<0.001 ***	OP_r	0.741	PaCiG_l	<0.001 ***
PaCiG_r	<0.001 ***	Pal_l	0.006 **	PaCiG_r	0.020 *	Pal_l	0.282
Pal_r	1.000	PC	0.862	Pal_r	0.028 *	PC	1.000
pITG_l	0.006 **	pITG_r	<0.001 ***	pITG_l	0.142	pITG_r	0.111
pMTG_l	0.011 *	pMTG_r	0.079	pMTG_l	1.000	pMTG_r	0.018 *
PO_l	1.000	PO_r	1.000	PO_l	0.034 *	PO_r	0.021 *
PostCG_l	0.003 **	PostCG_r	1.000	PostCG_l	1.000	PostCG_r	0.010 **
PP_l	1.000	PP_r	0.615	PP_l	0.701	PP_r	0.062
PreCG_l	<0.001 ***	PreCG_r	0.024 *	PreCG_l	0.024 *	PreCG_r	1.000
PrCun	<0.001 ***	pPaHC_l	1.000	PrCun	1.000	pPaHC_l	1.000
pPaHC_r	0.009 **	pSMG_l	1.000	pPaHC_r	0.142	pSMG_l	0.032 *
pSMG_r	0.168	pSTG_l	0.010 **	pSMG_r	<0.001 ***	pSTG_l	0.058

pSTG_r	0.480	PT_l	0.112	pSTG_r	0.028 *	PT_l	0.803
PT_r	0.271	pTFusC_l	0.112	PT_r	0.019 *	pTFusC_l	0.753
pTFusC_r	<0.001 ***	Pu_l	1.000	pTFusC_r	0.100	Pu_l	0.516
Pu_r	0.074	SCC_l	0.529	Pu_r	1.000	SCC_l	0.058
SCC_r	1.000	SFG_l	<0.001 ***	SCC_r	0.058	SFG_l	<0.001 ***
SFG_r	0.010 **	sLOC_l	<0.001 ***	SFG_r	0.073	sLOC_l	1.000
sLOC_r	<0.001 ***	SMA_l	0.592	sLOC_r	0.118	SMA_l	0.018 *
SMA_r	0.077	SPL_l	0.427	SMA_r	0.106	SPL_l	1.000
SPL_r	1.000	SubCalC	<0.001 ***	SPL_r	0.018 *	SubCalC	0.105
Tha_l	<0.001 ***	Tha_r	<0.001 ***	Tha_l	0.031 *	Tha_r	0.803
TOFusC_l	<0.001 ***	TOFusC_r	0.128	TOFusC_l	1.000	TOFusC_r	1.000
toITG_l	<0.001 ***	toITG_r	1.000	toITG_l	1.000	toITG_r	<0.001 ***
toMTG_l	1.000	toMTG_r	0.045 *	toMTG_l	0.164	toMTG_r	0.044 *
TP_l	1.000	TP_r	1.000	TP_l	0.904	TP_r	1.000
Ver12	0.306	Ver3	0.516	Ver12	0.044 *	Ver3	0.919
Ver45	0.005 **	Ver6	1.000	Ver45	1.000	Ver6	0.128
Ver7	0.482	Ver8	<0.001 ***	Ver7	0.018 *	Ver8	0.577
Ver9	<0.001 ***	Ver10	<0.001 ***	Ver9	0.024 *	Ver10	0.055
aITG_l	<0.001 ***	aITG_r	<0.001 ***	aITG_l	0.058	aITG_r	0.044 *
aMTG_l	0.038 *	aMTG_r	0.001 **	aMTG_l	0.038 *	aMTG_r	0.042 *

Results are relative to the Mann-Whitney or independent samples t-tests. They are reported in terms of p-value, after performing the Benjamini-Yekutieli correction (< 0.05, ** < 0.01, *** < 0.001). The 22 significant parcels common to both the ResNet18 and BC-GCN-SE models are highlighted in green.*

Table S3. List ordered by ranking of the 15% of parcels characterized by the highest RV for the classification of AD and HC subjects obtained using ResNet18 and BC-GCN-SE.

ResNe18		BC-GCN-SE	
AD	HC	AD	HC
Cereb10_l	Ver10	PreCG_r	BSt
Cereb10_r	Cereb10_l	pSMG_r	Cereb9_r
Ver10	PaCiG_r	PaCiG_l	Cereb9_l

aTFusC_l	PaCiG_l	OFusG_r	Cereb2_r
aTFusC_r	MedFC	Cereb1_r	Cereb8_r
FOrb_l	Cereb10_r	ICC_r	PostCG_r
aITG_r	FP_l	SPL_r	Cereb8_l
FOrb_r	FOrb_l	Tha_l	FP_r
SubCalC	FP_r	Ver10	Cereb2_l
aITG_l	FOrb_r	Cereb9_l	PreCG_r
Ver12	CO_r	Cereb8_r	Cereb45_r
CO_r	IFG_oper_l	Cereb9_r	Cereb45_l
aPaHC_l	IFG_oper_r	toITG_r	TOFusC_r
pSTG_r	IFG_tri_r	pSMG_l	PrCun
pITG_r	IFG_tri_l	Ver9	Cereb6_l
PO_l	aSTG_r	Cereb10_l	SFG_r
MedFC	FO_r	PaCiG_r	MidFG_r
Ver3	PO_l	pMTG_r	Hip_l
pSTG_l	MidFG_l	iLOC_r	Cereb7_l
aPaHC_r	pSTG_r	pSTG_r	Cereb1_l

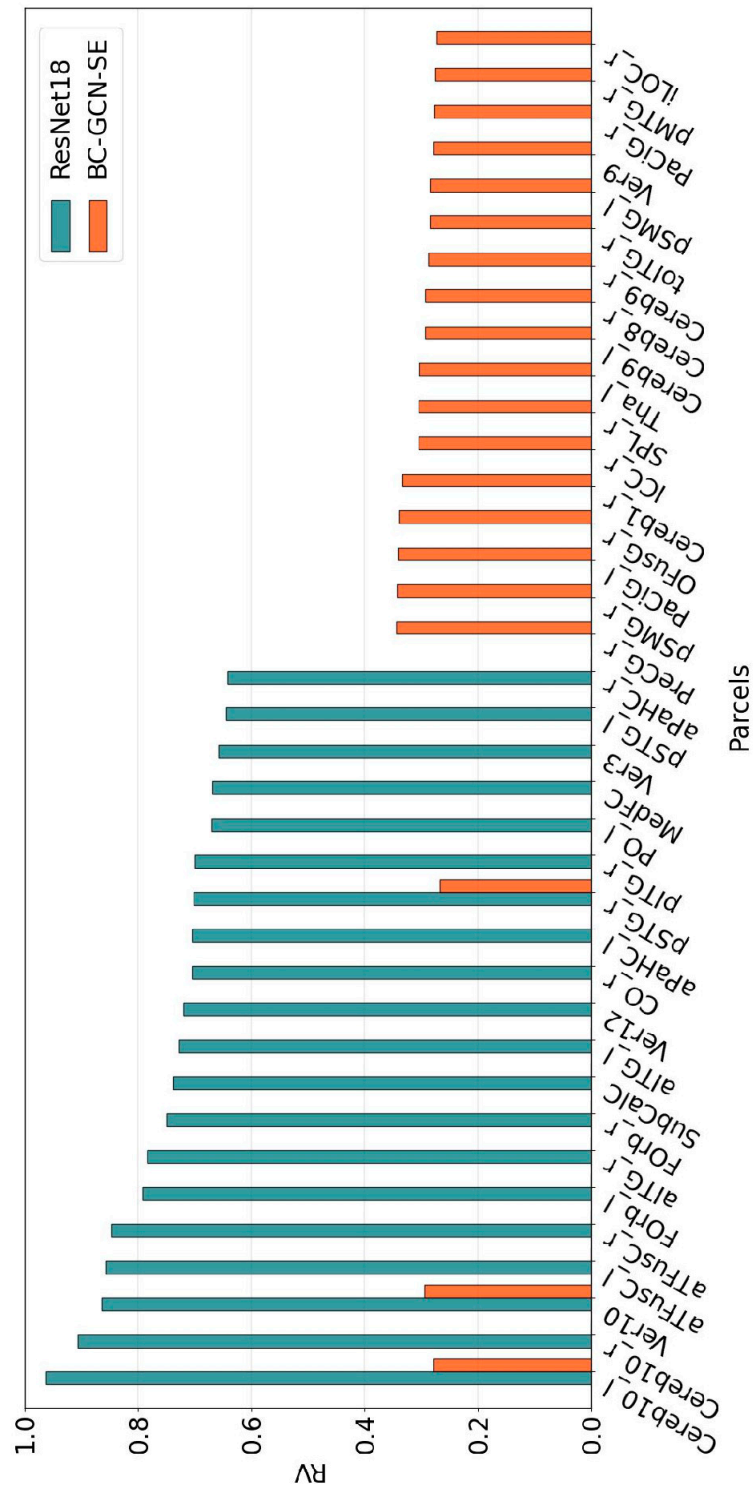


Figure S1. Comparative visualization of the Grad-CAM based RV measure for the most relevant brain parcels (top 15% – specified on the x axis) identified by ResNet18 (turquoise bars) and BC-GCN-SE (orange bars) for the AD classification. For visualization purposes all data are normalized between 0 and 1 using the minimum and the maximum Grad-CAM based RV measures obtained across every parcel for every subject correctly classified using the corresponding model.